

Stratospheric Circulation Changes Associated with the Hunga Tonga-Hunga Ha’apai Eruption

Lawrence Coy¹, P A Newman², K Wargan², G Partyka², S Strahan², and S Pawson²

¹NASA GSFC, SSAI

²NASA GSFC

September 13, 2022

Abstract

The 15 January 2022 eruption of the Hunga Tonga-Hunga Ha’apai underwater volcano injected a record amount of water directly into the stratosphere. This study attempts to quantify this impact on the temperature, as well as the subsequent changes to the stratospheric circulation, during the months following the eruption based on reanalysis fields. The extreme nature of the temperature, wind, and circulation changes are tracked through comparisons of the first six months of 2022 with the past 42 years. Examination of the data assimilation process shows that at 20 hPa the thermal observations are forcing temperatures to cool significantly, compensating for the absence of the excess stratospheric moisture in the model used for the reanalysis, resulting in unusually low temperatures. In response to this cooling the atmosphere adjusts by creating strong westerly winds above the temperature anomaly and large changes to the downward and poleward mean meridional circulation.

L. Coy^{1,2}, P. A. Newman¹, K. Wargan^{1,2}, G. Partyka^{1,2}, S. Strahan^{1,3}, and S. Pawson¹

¹NASA GSFC, Greenbelt, MD, USA.

²SSAI, Lanham, MD, USA.

³University of Maryland Baltimore County, Baltimore, MD, USA.

Corresponding author: Lawrence Coy (lawrence.coy@nasa.gov)

Key Points:

- Extreme perturbations in the stratospheric winds and temperatures are linked to a volcanic eruption.
- Hunga Tonga-Hunga Ha’apai eruption effects are unique in the stratospheric record.
- Data assimilation can track temperature and wind perturbations, even when some physics is missing.

Abstract

The 15 January 2022 eruption of the Hunga Tonga-Hunga Ha’apai underwater volcano injected a record amount of water directly into the stratosphere. This study attempts to quantify this impact on the temperature, as well as the subsequent changes to the stratospheric circulation, during the months following the eruption based on reanalysis fields. The extreme nature of the temperature, wind, and circulation changes are tracked through comparisons of the first six months of 2022 with the past 42 years. Examination of the data assimilation process shows that at 20 hPa the thermal observations are forcing temperatures to cool significantly, compensating for the absence of the excess stratospheric moisture in the model used for the reanalysis, resulting in unusually low temperatures. In response to this cooling the atmosphere adjusts by creating strong westerly winds above the temperature anomaly and large changes to the downward and poleward mean meridional circulation.

Plain Language Summary

The 15 January 2022 eruption of the Hunga Tonga-Hunga Ha’apai underwater volcano injected a record amount of water directly into the stratosphere. This study attempts to quantify this impact on the temperature, as well as the subsequent changes to the stratospheric circulation, during the months following the eruption. The extreme nature of the stratospheric temperature, wind, and circulation changes are tracked through comparisons of the first six months of 2022 with the past 42 years. Details of the stratospheric perturbations in latitude and pressure are presented for June 2022, where anomalously low temperatures are found at near 20 km altitude from 60°S to 30°S. In response to this cooling the atmosphere adjusts by creating strong westerly winds above the temperature anomaly and large changes to the downward and poleward mean meridional circulation.

1 Introduction

The 15 January 2022 eruption of the Hunga Tonga-Hunga Ha’apai underwater volcano injected an unprecedented amount of water directly into the stratosphere (Millán et al., 2022; Xu et al., 2022; Carr et al., 2022). While the initial injection plume at 20°S reached to the upper stratosphere (Carr et al., 2022), Millán et al. (2022), showed that after three months this excess water vapor settled near 20 hPa altitude in a latitude band from 30°S to 5°N. With no major thermodynamic or photochemical sinks, this excess moisture is expected to remain in the stratosphere for two to three years. Water vapor is radiatively active in the infrared, contributing to the total radiative cooling in the stratosphere, which is dominated by the effects of carbon dioxide and ozone (e.g., Gille and Lyjak, 1986). These large perturbations in water vapor are expected to increase the amount of radiation lost to space, locally cooling the stratosphere. This study attempts to quantify this impact on the temperature, as well as the subsequent changes to the stratospheric circulation, during the first six months after the eruption.

The MERRA-2 (Modern-Era Retrospective Analysis for Research and Applications, Version 2) reanalysis (Gelaro et al., 2017) provides the circulation fields (temperatures and winds) for this study. While MERRA-2 assimilates a number of in-situ and space-based observations that constrain tropospheric moisture, stratospheric water vapor observations are not assimilated. Stratospheric moisture is closely constrained to monthly climatologies imposed by a relaxation constraint in the GEOS model, so that the stratospheric water vapor in MERRA-2 does not respond to the volcanic perturbation. This precludes the use of MERRA-2 to directly infer the thermal impacts of the water vapor increase on the circulation. However, numerous nadir- and limb-sounding microwave observations are assimilated in the stratosphere (McCarty et al., 2016) and these data will constrain the analyzed temperatures, which can be used to indirectly infer the thermal and dynamical response of the stratosphere in MERRA-2. Additionally, a more recent data assimilation system, M2-SCREAM (described below), does contain additional water vapor and is used to compare with the MERRA-2 analysis and radiative temperature tendencies.

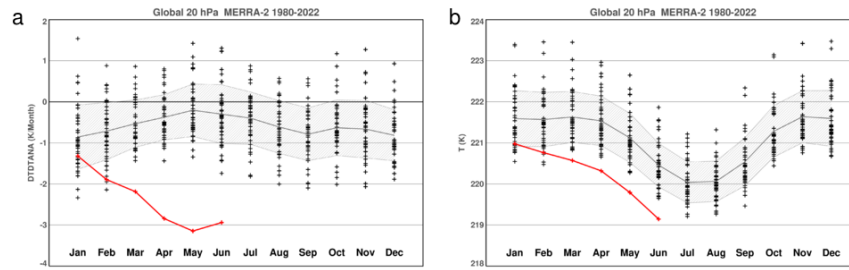
2 Assimilation Products

The 43-year (1980-2022) climate record from MERRA-2 is used to assess the anomalies of 2022. Two sets of monthly averaged files are used: The assimilation files for winds and temperatures (GMAO, 2015a), and the temperature tendency files to obtain the analysis temperature tendencies (GMAO, 2015b). The residual zonal mean circulations for each month are calculated from the monthly averaged assimilation files as, in addition to winds and temperatures, these files also contain the heat and momentum fluxes needed for evaluation of the residual circulation (see Andrews et al., 1987, page 128). For this study we examine the stream function of the residual circulation as well as the residual mean meridional and vertical winds.

The MERRA-2 Stratospheric Composition Reanalysis of Aura Microwave Limb Sounder (M2-SCREAM: Wargan et al., 2022) is a new stratosphere-focused reanalysis product developed at NASA’s Global Modeling and Assimilation Office. M2-SCREAM assimilates stratospheric profiles of ozone, water vapor, hydrogen chloride, nitric acid, and nitrous oxide from version 4.2 retrievals of the Microwave Limb Sounder (MLS: Waters et al., 2006; Livesey et al., 2020) observations, the same as those used in Millán et al. (2022), alongside total ozone observations from the Ozone Monitoring Instrument (Levelt et al., 2006, 2018). Temperature,

winds, surface pressure, and tropospheric water vapor in M2-SCREAM are constrained by the MERRA-2 assimilated fields. M2-SCREAM covers the MLS period from September 2004 to May 2022. Details of the M2-SCREAM system are described in Wargan et al., (2020; 2022). Because this reanalysis assimilates MLS data, unlike MERRA-2, it contains a representation of the water vapor enhancement from the Hunga Tonga eruption in agreement with MLS. The total increase of stratospheric water vapor mass calculated from M2-SCREAM is 10% as in Millán et al. (2022). As shown below, the radiative transfer model in M2-SCREAM responds to the moisture enhancement by producing long wave cooling in better agreement with the observations.

3 Results



The assimilation technique in MERRA-2 imposes an additional forcing, the analysis tendency, to force the GEOS model towards the observations. This additional forcing can often be regarded as a compensation for inadequacies in the representation of processes in the model, and can manifest as either random error (with a complex spatial structure) or as a mean bias, with a coherent spatio-temporal structure. Because the GEOS model uses climatological water vapor fields in the stratosphere of MERRA-2, any anomalous radiative forcing caused by the volcanic eruption will not be captured in the radiative tendencies, and will instead be captured by the bias in the analysis tendency term. The global analysis temperature tendencies at 20hPa, shown for each month of MERRA-2 (Fig. 1a), reveals the anomalous values seen in 2022. Cooling by the increments is below average in January 2022, one of the strongest cooling years in February, and lies well below the average in March through June. In May 2022 the cooling is over three standard deviations below the mean. These anomalies at 20 hPa coincide with the peak moisture anomaly isolated in Millán et al. (2022), are the largest in MERRA-2. The increments show weaker additional cooling at 10hPa and weak additional warming at 30hPa (not shown).

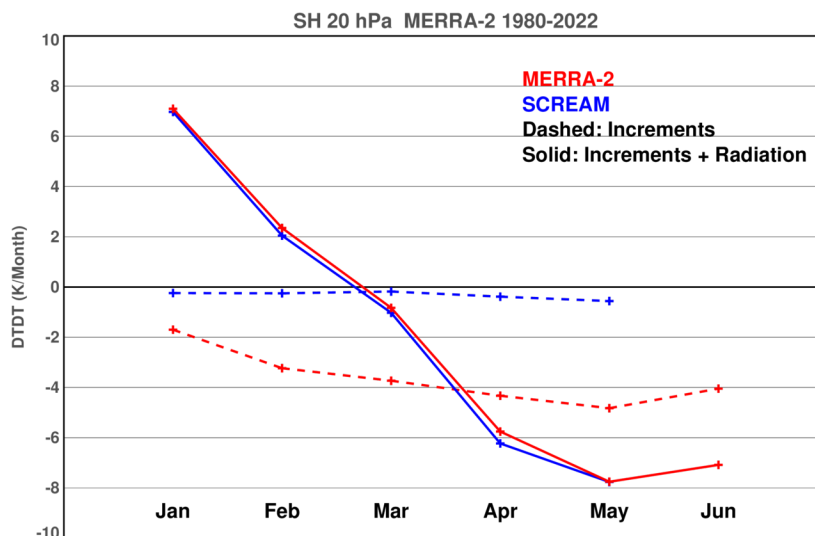


Figure 2: The 20 hPa monthly and Southern Hemisphere averaged MERRA-2 temperature increments (red dashed), MERRA-2 sum of temperature increments and radiative tendency (red solid), M2-SCREAM temperature increments (blue dashed), and SCREAM sum of temperature increments and radiative tendency (blue solid).

The global temperature at 20 hPa (Fig. 1b) depicts the cooler than average global temperatures associated with the record cold increments during January through June 2022. The January temperatures are approximately one standard deviation below average, the February temperatures continue to cool, while the March through June temperatures are setting new records for cold global temperatures at 20 hPa. Note that the temperature increments can suggest temperatures larger than the temperature departures. For example, in June 2022 the temperature increments are nearly 3 K/month below the mean, while the temperatures for the month are only ~1.25 K below average indicating the importance of the other terms, such as dynamical forcing and radiative transfer, in determining temperature. Nevertheless, these record cold increments are associated with the record low temperatures.

More evidence that the anomalous increments correspond to expected anomalous water vapor is provided by M2-SCREAM temperature tendency fields (Fig. 2). These are shown averaged over the Southern Hemisphere (SH) rather than globally as the global averaged summed temperature tendencies are much smaller. The M2-SCREAM system's smaller magnitude temperature increments than MERRA-2 (dashed curves) show that M2-SCREAM can respond radiatively to the water vapor anomaly without a strong reliance on the temperature observations. However, when the analysis and radiative tendencies are summed (solid curves), both systems show similar temperature tendencies indicating that the MERRA-2 increments are replacing the additional water vapor portion of the radiative tendency.

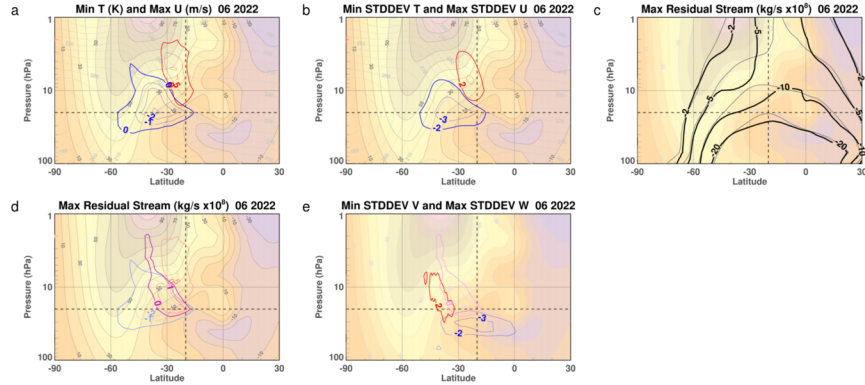


Figure 3 Cross sections for June showing zonal mean zonal winds (10 m/s, filled contours) and temperatures (5K, gray contours (a and b): a) Blue contours: record cold regions where the contours (1 K) denote how much June 2022 is below the previous record low temperature. Red contours: record strong zonal mean winds where the contours (5 m/s) denote how much June 2022 is above the previous record strong wind; b) Blue contours: standard deviations of temperature below the mean (contour interval of 1, starting at -2) and red contours: standard deviations of zonal wind above the mean (contour interval of 1, starting at 2); c) Residual mean stream function ($-2, -5, -10, -20 \times 10^8$ kg/s) for 1980-2021 average (gray) and 2022 (black); d) residual mean circulation stream function greater than the past maximum value (magenta, contour interval 1×10^8 kg/s) with wind and temperature record as in a); e) Blue contours: standard deviations of residual mean meridional wind below the mean (contour levels of -3 and -2) and red contours: standard deviations of residual mean vertical velocity above the mean (contour level of 2). Dashed lines denote 20°S and 20 hPa.

This cooling is not uniform over the globe but is strongest near 30°S and 20 hPa. In June 2022 record low temperatures for the month stretch from 55°S to 15°S (Fig. 3a). These temperatures break the previous low temperature record by as much as 3K. In addition, the zonal mean winds are breaking records by as much as 10 m/s. The location of these record strong winds near the low temperatures is consistent with the geostrophic relation where increased cooling toward the pole requires increased vertical wind shear. In addition to setting records for the month of June, these 2022 low temperatures and strong winds were outside the standard deviation of the year-to-year variability (Fig. 3b) with values greater than double the standard deviation.

These wind and temperature anomalies are likely associated with changes in the mean circulation as the atmosphere adjusts to the temperature perturbation. The counter-clockwise flow of the residual mean stream function for 2022 (Fig. 3c) shows large distortions in the region near the wind and temperature anomalies compared to the 1980-2022 averaged June residual mean stream function. In particular, the strong vertical gradient in the stream function at 30°S and 30 hPa denotes a stronger than average poleward (negative) flow in 2022. This can be represented as a clockwise anomaly in the residual mean stream function (Fig. 3d). In Fig. 3d, the stream function plotted is greater than any of the previous years in that region. This means that the distortion of the stream function from the mean seen in Fig. 3c is larger than in previous years.

The residual mean circulation can also be expressed in terms of residual mean meridional and vertical velocities (Fig. 3e). The residual mean meridional velocity is particularly striking with negative (poleward) values over three standard deviations below the mean from 10°S - 30°S near 30 hPa. The upward mean vertical wind anomalies are over two standard deviations above the mean on the poleward side of the stream function anomaly. This upward anomaly does not correspond to an actual upward circulation but expresses the weaker downward circulation than average as seen in the nearly horizontal stream function regions in Fig. 3c.

4 Conclusions

Anomalous temperatures and circulation patterns analyzed by MERRA-2 in the southern hemisphere during

June 2022 can be forensically attributed to the stratospheric water vapor injection from the January 2022 eruption of the Hunga Tonga-Hunga Ha’apai underwater volcano. These anomalies can be traced back to March 2022. Their consistency in space and time suggests a realistic response to a geophysical event rather than a yearly random dynamical fluctuation. In June the record winds are part of an unusual secondary jet maximum at 10 hPa, 30°S-20°S.

These wind and temperature anomalies (Fig. 3a, b) develop from the assimilation of data, mainly routine, satellite based, nadir viewing radiometers and geostrophic balance and are likely to be very realistic. Note that MERRA-2 does assimilate MLS temperatures, but only at pressures of 5hPa and lower. The residual mean circulation might be more difficult to interpret. If the cooling analysis temperature increments mainly reflect the missing water vapor cooling then they can be considered to be the missing cooling term from the lack of stratospheric water vapor in the assimilation system. Then the calculated residual circulation (Fig. 3c, d, e) should realistically capture the perturbed residual circulation. If, however, the analysis temperature increments also contain cooling induced by circulations in the atmosphere’s response to the water vapor perturbation, then it is possible that the residual circulation may adjust in an unphysical manner. However, the good SH 20 hPa agreement between MERRA-2 and M2-SCREAM seen in the sum of the analysis and radiative temperature tendencies (Fig. 2) suggests that the MERRA-2 analysis tendencies are representative of the missing water vapor cooling. Future work is planned for model simulations that include a realistic representation of the stratospheric water perturbations. These calculations should provide a more complete picture of the atmospheric response to the volcanic perturbation.

Acknowledgments

This work was supported by NASA MAP and ACMAP programs. Resources supporting this work were provided by the NASA High-End Computing (HEC) Program through the NASA Center for Climate Simulation (NCCS) at Goddard Space Flight Center.

Open Research

The MERRA-2 products are available on the NASA Goddard Earth Sciences Data and Information Services Center (GES DISC). Specific MERRA-2 product collections used here are cited appropriately in the references. The 2022 temperature tendencies from M2-SCREAM are available from <https://gmao.gsfc.nasa.gov/gmaoftp/STRATOSPHERE/M2-SCREAM/T-tendencies/>. Historical M2-SCREAM output can be accessed from <https://disc.gsfc.nasa.gov/datasets?keywords=m2-scream&page=1>.

References

- Andrews, D. G., Holton, J. R., and Leovy, C. B. (1987), *Middle Atmosphere Dynamics*, Academic Press, 489pp.
- Carr, J. L., Horváth, Á., Wu, D. L., & Friberg, M. D. (2022). Stereo plume height and motion retrievals for the record-setting Hunga Tonga-Hunga Ha’apai eruption of 15 January 2022. *Geophysical Research Letters*, 49, e2022GL098131. <https://doi.org/10.1029/2022GL098131>
- Gelaro, R., McCarty, W., Suárez, M. J., Todling, R., Molod, A., Takacs, L., Randles, C. A., Darmenov, A., Bosilovich, M. G., Reichle, R., Wargan, K., Coy, L., Cullather, R., Draper, C., Akella, S., Buchard, V., Conaty, A., da Silva, A. M., Gu, W., Kim, G., Koster, R., Lucchesi, R., Merkova, D., Nielsen, J. E., Partyka, G., Pawson, S., Putman, W., Rienecker, M., Schubert, S. D., Sienkiewicz, M., & Zhao, B. (2017). The Modern-Era Retrospective Analysis for Research and Applications, Version 2 (MERRA-2), *Journal of Climate*, 30 (14), 5419-5454. Retrieved Jul 27, 2022, from <https://journals.ametsoc.org/view/journals/clim/30/14/jcli-d-16-0758.1.xml>
- Gille, J.C., and L.V. Lyjak (1986). Radiative Heating and Cooling Rates in the Middle Atmosphere. *J. Atmos. Sci.*, 43(20), 2215-2229. DOI: [https://doi.org/10.1175/1520-0469\(1986\)043<2215:RHACRI>2.0.CO;2](https://doi.org/10.1175/1520-0469(1986)043<2215:RHACRI>2.0.CO;2)
- Global Modeling and Assimilation Office (GMAO) (2022), M2-SCREAM: 3d,3-Hourly,Instantaneous,Model-Level,Assimilation,Assimilated Constituent Fields,Replayed MERRA-2 Meteorological Fields, Greenbelt,

MD, USA, Goddard Earth Sciences Data and Information Services Center (GES DISC), Accessed: July 2022, doi:10.5067/7PR3XRD6Q3NQ

Global Modeling and Assimilation Office (GMAO) (2015a), MERRA-2 instM_3d_asm_Np: 3d,Monthly mean,Instantaneous,Pressure-Level,Assimilation,Assimilated Meteorological Fields V5.12.4, Greenbelt, MD, USA, Goddard Earth Sciences Data and Information Services Center (GES DISC), Accessed: **Jul 27, 2022**, 10.5067/2E096JV59PK7

Global Modeling and Assimilation Office (GMAO) (2015b), MERRA-2 tavgM_3d_tdt_Np: 3d,Monthly mean,Time-Averaged,Pressure-Level,Assimilation,Temperature Tendencies V5.12.4, Greenbelt, MD, USA, Goddard Earth Sciences Data and Information Services Center (GES DISC), Accessed: **Jul 27, 2022**, 10.5067/VILT59HI2MOY

Levelt, P. F., van den Oord, G. H. J., Dobber, M. R., Mälkki, A., Visser, H., Vries, J. D., Stammes, P., Lundell, J. O. V., and Saari, H. (2006). The Ozone Monitoring Instrument, *IEEE Trans. Geosci. Remote Sens.*, 44, 1093–1101, <https://doi.org/10.1109/TGRS.2006.872333>.

Levelt, P. F., Joiner, J., Tamminen, J., Veefkind, J. P., Bhartia, P. K., Stein Zweers, D. C., Duncan, B., et al. (2018). The Ozone Monitoring Instrument: overview of 14 years in space, *Atmos. Chem. Phys.*, 18, 5699–5745, <https://doi.org/10.5194/acp-18-5699-2018>.

Livesey, N. J., Read, W. G., Wagner, P. A., Froidevaux, L., Lambert, A., Manney, G. L. et al. (2020). Version 4.2x Level 2 and 3 data quality and description document, JPL D-33509 Rev. E. Retrieved from https://mls.jpl.nasa.gov/data/v4-2_data_quality_document.pdf, 2020

McCarty, Will, Lawrence Coy, Ronald Gelaro, Albert Huang, Dagmar Merkova, Edmond B. Smith, Meta Seinkiewicz, and Krzysztof Wargan (2016). MERRA-2 Input Observations: Summary and Assessment. NASA Technical Report Series on Global Modeling and Data Assimilation, NASA/TM-2016-104606, Vol. 46, 61 pp. Document (3553 kB).

Millán, L., Santee, M. L., Lambert, A., Livesey, N. J., Werner, F., Schwartz, M. J., et al. (2022). The Hunga Tonga-Hunga Ha’apai Hydration of the Stratosphere. *Geophysical Research Letters*, 49, e2022GL099381. <https://doi.org/10.1029/2022GL099381>

Sellitto P, Podglajen A, Belhadji R, et al. The unexpected radiative impact of the Hunga Tonga eruption of January 15th, 2022. *Research Square*; 2022. DOI: 10.21203/rs.3.rs-1562573/v1.

Wargan, K., Weir, B., Manney, G. L., Cohn, S. E., K.E. Knowland, P. Wales & Livesey, N. J. (2022). M2-SCREAM: A Stratospheric Composition Reanalysis of Aura MLS data with MERRA-2 transport. *Earth Sys. Sci. Dat.*, submitted.

Wargan, K., Weir, B., Manney, G. L., Cohn, S. E., & Livesey, N. J. (2020). The anomalous 2019 Antarctic ozone hole in the GEOS Constituent Data Assimilation System with MLS observations. *Journal of Geophysical Research: Atmospheres*, 125, e2020JD033335. <https://doi.org/10.1029/2020JD033335>.

Waters, J. W., Froidevaux, L., Harwood, R.S., Jarnot, R.F., Pickett, H.M., Read, W.G. et al. (2006). The Earth Observing System Microwave Limb Sounder (EOS MLS) on the Aura satellite. *IEEE Trans. Geosci. Remote Sens.*, 44, 1075–1092. <https://doi.org/10.1109/TGRS.2006.873771>.

Xu, J., Li, D., Bai, Z., Tao, M., Bian, J. (2022) Large Amounts of Water Vapor Were Injected into the Stratosphere by the Hunga Tonga–Hunga Ha’apai Volcano Eruption. *Atmosphere*, 13, 912. <https://doi.org/10.3390/atmos13060912>.

1 **Stratospheric Circulation Changes Associated with the Hunga Tonga-Hunga Ha'apai**
2 **Eruption**

3 **L. Coy^{1,2}, P. A. Newman¹, K. Wargan^{1,2}, G. Partyka^{1,2}, S. Strahan^{1,3}, and S. Pawson¹**

4 ¹NASA GSFC, Greenbelt, MD, USA.

5 ²SSAI, Lanham, MD, USA.

6 ³University of Maryland Baltimore County, Baltimore, MD, USA.

7 Corresponding author: Lawrence Coy (lawrence.coy@nasa.gov)

8 **Key Points:**

- 9 • Extreme perturbations in the stratospheric winds and temperatures are linked to a
10 volcanic eruption.
- 11 • Hunga Tonga-Hunga Ha'apai eruption effects are unique in the stratospheric record.
- 12 • Data assimilation can track temperature and wind perturbations, even when some physics
13 is missing.
- 14

15 **Abstract**

16

17 The 15 January 2022 eruption of the Hunga Tonga-Hunga Ha'apai underwater volcano
18 injected a record amount of water directly into the stratosphere. This study attempts to quantify
19 this impact on the temperature, as well as the subsequent changes to the stratospheric circulation,
20 during the months following the eruption based on reanalysis fields. The extreme nature of the
21 temperature, wind, and circulation changes are tracked through comparisons of the first six
22 months of 2022 with the past 42 years. Examination of the data assimilation process shows that
23 at 20 hPa the thermal observations are forcing temperatures to cool significantly, compensating
24 for the absence of the excess stratospheric moisture in the model used for the reanalysis,
25 resulting in unusually low temperatures. In response to this cooling the atmosphere adjusts by
26 creating strong westerly winds above the temperature anomaly and large changes to the
27 downward and poleward mean meridional circulation.

28

29 **Plain Language Summary**

30 The 15 January 2022 eruption of the Hunga Tonga-Hunga Ha'apai underwater volcano injected a
31 record amount of water directly into the stratosphere. This study attempts to quantify this impact
32 on the temperature, as well as the subsequent changes to the stratospheric circulation, during the
33 months following the eruption. The extreme nature of the stratospheric temperature, wind, and
34 circulation changes are tracked through comparisons of the first six months of 2022 with the past
35 42 years. Details of the stratospheric perturbations in latitude and pressure are presented for June
36 2022, where anomalously low temperatures are found at near 20 km altitude from 60°S to 30°S.
37 In response to this cooling the atmosphere adjusts by creating strong westerly winds above the
38 temperature anomaly and large changes to the downward and poleward mean meridional
39 circulation.

40 **1 Introduction**

41 The 15 January 2022 eruption of the Hunga Tonga-Hunga Ha'apai underwater volcano
42 injected an unprecedented amount of water directly into the stratosphere (Millán et al., 2022; Xu
43 et al., 2022; Carr et al., 2022). While the initial injection plume at 20°S reached to the upper
44 stratosphere (Carr et al., 2022), Millán et al. (2022), showed that after three months this excess
45 water vapor settled near 20 hPa altitude in a latitude band from 30°S to 5°N. With no major
46 thermodynamic or photochemical sinks, this excess moisture is expected to remain in the
47 stratosphere for two to three years. Water vapor is radiatively active in the infrared, contributing
48 to the total radiative cooling in the stratosphere, which is dominated by the effects of carbon
49 dioxide and ozone (e.g., Gille and Lyjak, 1986). These large perturbations in water vapor are
50 expected to increase the amount of radiation lost to space, locally cooling the stratosphere. This
51 study attempts to quantify this impact on the temperature, as well as the subsequent changes to
52 the stratospheric circulation, during the first six months after the eruption.

53 The MERRA-2 (Modern-Era Retrospective Analysis for Research and Applications,
54 Version 2) reanalysis (Gelaro et al., 2017) provides the circulation fields (temperatures and
55 winds) for this study. While MERRA-2 assimilates a number of in-situ and space-based
56 observations that constrain tropospheric moisture, stratospheric water vapor observations are not
57 assimilated. Stratospheric moisture is closely constrained to monthly climatologies imposed by a

58 relaxation constraint in the GEOS model, so that the stratospheric water vapor in MERRA-2
59 does not respond to the volcanic perturbation. This precludes the use of MERRA-2 to directly
60 infer the thermal impacts of the water vapor increase on the circulation. However, numerous
61 nadir- and limb-sounding microwave observations are assimilated in the stratosphere (McCarty
62 et al., 2016) and these data will constrain the analyzed temperatures, which can be used to
63 indirectly infer the thermal and dynamical response of the stratosphere in MERRA-2.
64 Additionally, a more recent data assimilation system, M2-SCREAM (described below), does
65 contain additional water vapor and is used to compare with the MERRA-2 analysis and radiative
66 temperature tendencies.

67 **2 Assimilation Products**

68 The 43-year (1980-2022) climate record from MERRA-2 is used to assess the anomalies
69 of 2022. Two sets of monthly averaged files are used: The assimilation files for winds and
70 temperatures (GMAO, 2015a), and the temperature tendency files to obtain the analysis
71 temperature tendencies (GMAO, 2015b). The residual zonal mean circulations for each month
72 are calculated from the monthly averaged assimilation files as, in addition to winds and
73 temperatures, these files also contain the heat and momentum fluxes needed for evaluation of the
74 residual circulation (see Andrews et al., 1987, page 128). For this study we examine the stream
75 function of the residual circulation as well as the residual mean meridional and vertical winds.

76 The MERRA-2 Stratospheric Composition Reanalysis of Aura Microwave Limb Sounder (M2-
77 SCREAM: Wargan et al., 2022) is a new stratosphere-focused reanalysis product developed at
78 NASA's Global Modeling and Assimilation Office. M2-SCREAM assimilates stratospheric
79 profiles of ozone, water vapor, hydrogen chloride, nitric acid, and nitrous oxide from version 4.2
80 retrievals of the Microwave Limb Sounder (MLS: Waters et al., 2006; Livesey et al., 2020)
81 observations, the same as those used in Millán et al. (2022), alongside total ozone observations
82 from the Ozone Monitoring Instrument (Levelt et al., 2006, 2018). Temperature, winds, surface
83 pressure, and tropospheric water vapor in M2-SCREAM are constrained by the MERRA-2
84 assimilated fields. M2-SCREAM covers the MLS period from September 2004 to May 2022.
85 Details of the M2-SCREAM system are described in Wargan et al., (2020; 2022). Because this
86 reanalysis assimilates MLS data, unlike MERRA-2, it contains a representation of the water
87 vapor enhancement from the Hunga Tonga eruption in agreement with MLS. The total increase
88 of stratospheric water vapor mass calculated from M2-SCREAM is 10% as in Millán et al.
89 (2022). As shown below, the radiative transfer model in M2-SCREAM responds to the moisture
90 enhancement by producing long wave cooling in better agreement with the observations.

91

92 **3 Results**

93 The assimilation technique in MERRA-2 imposes an additional forcing, the analysis
94 tendency, to force the GEOS model towards the observations. This additional forcing can often
95 be regarded as a compensation for inadequacies in the representation of processes in the model,
96 and can manifest as either random error (with a complex spatial structure) or as a mean bias, with
97 a coherent spatio-temporal structure. Because the GEOS model uses climatological water vapor
98 fields in the stratosphere of MERRA-2, any anomalous radiative forcing caused by the volcanic
99 eruption will not be captured in the radiative tendencies, and will instead be captured by the bias

100 in the analysis tendency term. The global analysis temperature tendencies at 20hPa, shown for
 101 each month of MERRA-2 (Fig. 1a), reveals the anomalous values seen in 2022. Cooling by the
 102 increments is below average in January 2022, one of the strongest cooling years in February, and
 103 lies well below the average in March through June. In May 2022 the cooling is over three
 104 standard deviations below the mean. These anomalies at 20 hPa coincide with the peak moisture

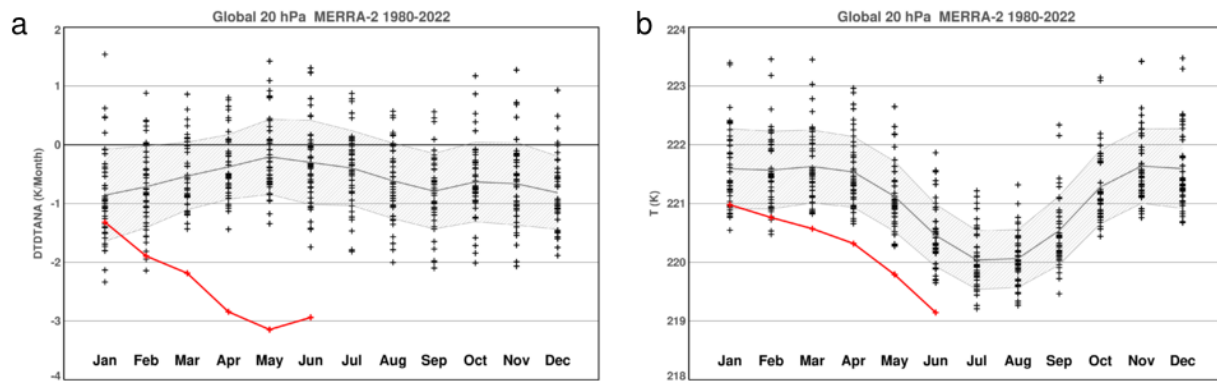
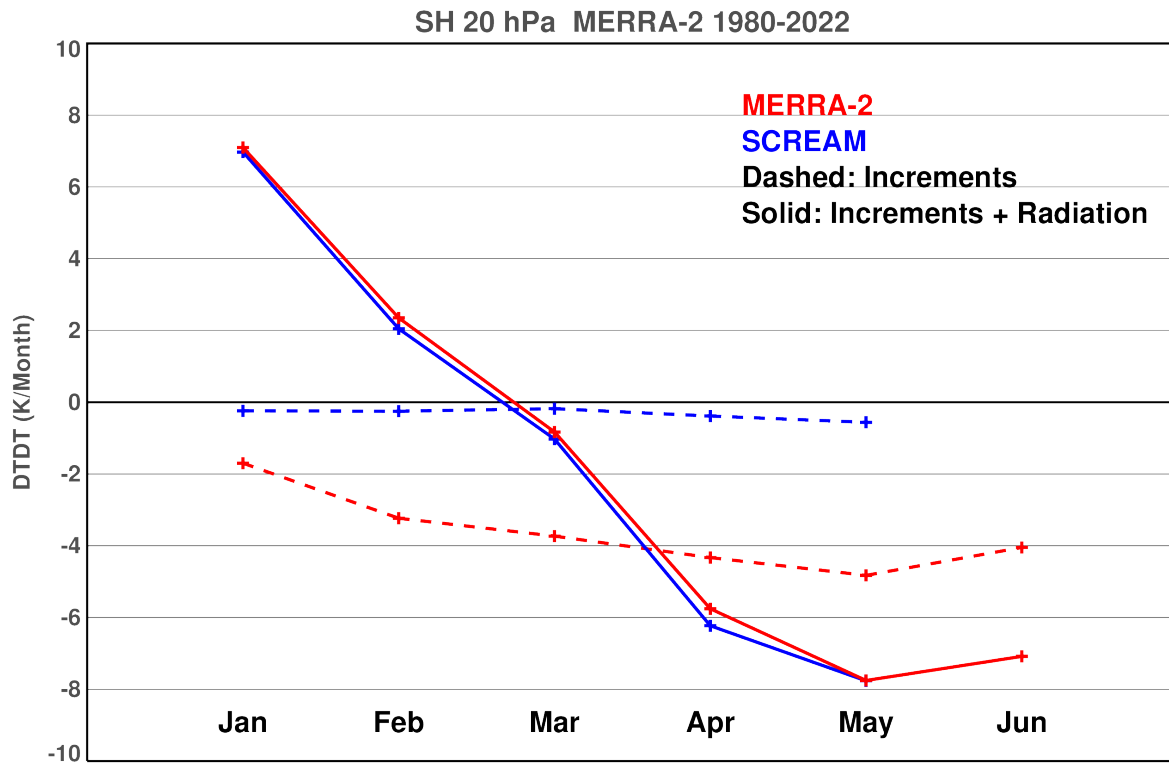


Figure 1: The monthly and globally averaged a) temperature increments and b) temperature at 20 hPa. The gray curve denotes the multi-year mean, the gray shading denotes the standard deviation for each month, and the red curve denotes the year 2022.

105 anomaly isolated in Millán et al. (2022), are the largest in MERRA-2. The increments show
 106 weaker additional cooling at 10hPa and weak additional warming at 30hPa (not shown).

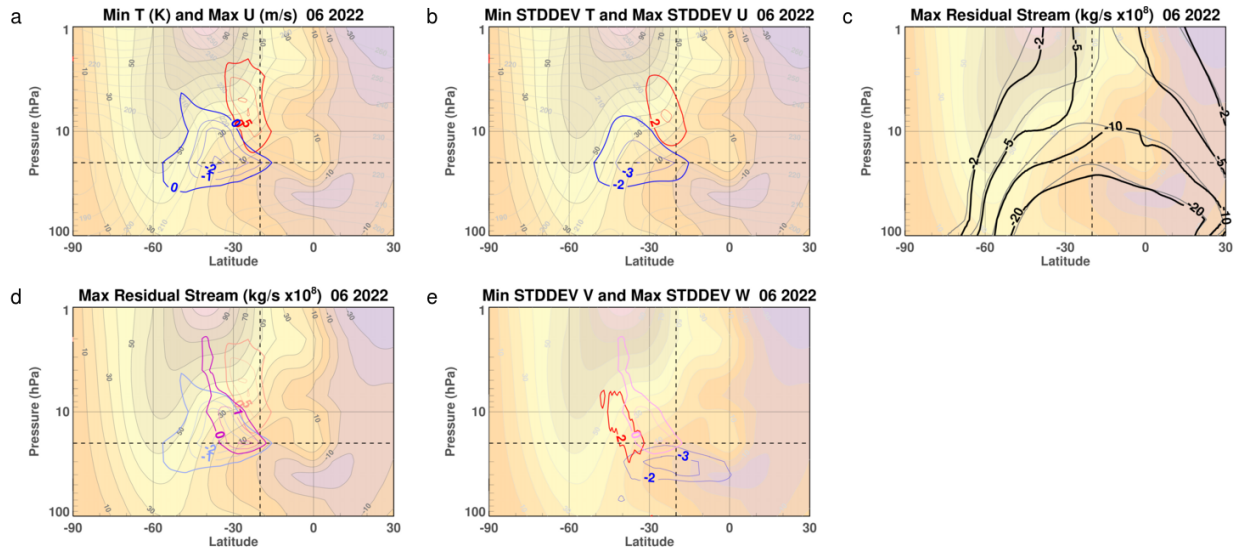


107
 108 *Figure 2: The 20 hPa monthly and Southern Hemisphere averaged MERRA-2 temperature*
 109 *increments (red dashed), MERRA-2 sum of temperature increments and radiative*
 110 *tendency (red solid), M2-SCREAM temperature increments (blue dashed), and SCREAM sum of temperature*
 111 *increments and radiative tendency (blue solid).*

112 The global temperature at 20 hPa (Fig. 1b) depicts the cooler than average global
 113 temperatures associated with the record cold increments during January through June 2022. The
 114 January temperatures are approximately one standard deviation below average, the February
 115 temperatures continue to cool, while the March through June temperatures are setting new
 116 records for cold global temperatures at 20 hPa. Note that the temperature increments can suggest
 117 temperatures larger than the temperature departures. For example, in June 2022 the temperature
 118 increments are nearly 3 K/month below the mean, while the temperatures for the month are only
 119 ~1.25 K below average indicating the importance of the other terms, such as dynamical forcing
 120 and radiative transfer, in determining temperature. Nevertheless, these record cold increments are
 121 associated with the record low temperatures.

122 More evidence that the anomalous increments correspond to expected anomalous water vapor is
 123 provided by M2-SCREAM temperature tendency fields (Fig. 2). These are shown averaged over
 124 the Southern Hemisphere (SH) rather than globally as the global averaged summed temperature
 125 tendencies are much smaller. The M2-SCREAM system's smaller magnitude temperature
 126 increments than MERRA-2 (dashed curves) show that M2-SCREAM can respond radiatively to

127 the water vapor anomaly without a strong reliance on the temperature observations. However,
 128 when the analysis and radiative tendencies are summed (solid curves), both systems show similar
 129 temperature tendencies indicating that the MERRA-2 increments are replacing the additional
 130 water vapor portion of the radiative tendency.



131
 132 *Figure 3 Cross sections for June showing zonal mean zonal winds (10 m/s, filled contours) and*
 133 *temperatures (5K, gray contours (a and b): a) Blue contours: record cold regions where the*
 134 *contours (1 K) denote how much June 2022 is below the previous record low temperature. Red*
 135 *contours: record strong zonal mean winds where the contours (5 m/s) denote how much June*
 136 *2022 is above the previous record strong wind; b) Blue contours: standard deviations of*
 137 *temperature below the mean (contour interval of 1, starting at -2) and red contours: standard*
 138 *deviations of zonal wind above the mean (contour interval of 1, starting at 2); c) Residual mean*
 139 *stream function (-2, -5, -10, -20 $\times 10^8$ kg/s) for 1980-2021 average (gray) and 2022 (black); d)*
 140 *residual mean circulation stream function greater than the past maximum value (magenta,*
 141 *contour interval 1×10^8 kg/s) with wind and temperature record as in a); e) Blue contours:*
 142 *standard deviations of residual mean meridional wind below the mean (contour levels of -3 and -*
 143 *2) and red contours: standard deviations of residual mean vertical velocity above the mean*
 144 *(contour level of 2). Dashed lines denote 20°S and 20 hPa.*

145 This cooling is not uniform over the globe but is strongest near 30°S and 20 hPa. In June
 146 2022 record low temperatures for the month stretch from 55°S to 15°S (Fig. 3a). These
 147 temperatures break the previous low temperature record by as much as 3K. In addition, the zonal
 148 mean winds are breaking records by as much as 10 m/s. The location of these record strong
 149 winds near the low temperatures is consistent with the geostrophic relation where increased
 150 cooling toward the pole requires increased vertical wind shear. In addition to setting records for
 151 the month of June, these 2022 low temperatures and strong winds were outside the standard
 152 deviation of the year-to-year variability (Fig. 3b) with values greater than double the standard
 153 deviation.

154 These wind and temperature anomalies are likely associated with changes in the mean
 155 circulation as the atmosphere adjusts to the temperature perturbation. The counter-clockwise

156 flow of the residual mean stream function for 2022 (Fig. 3c) shows large distortions in the region
157 near the wind and temperature anomalies compared to the 1980-2022 averaged June residual
158 mean stream function. In particular, the strong vertical gradient in the stream function at 30°S
159 and 30 hPa denotes a stronger than average poleward (negative) flow in 2022. This can be
160 represented as a clockwise anomaly in the residual mean stream function (Fig. 3d). In Fig. 2d,
161 the stream function plotted is greater than any of the previous years in that region. This means
162 that the distortion of the stream function from the mean seen in Fig. 3c is larger than in previous
163 years.

164 The residual mean circulation can also be expressed in terms of residual mean meridional
165 and vertical velocities (Fig. 3e). The residual mean meridional velocity is particularly striking
166 with negative (poleward) values over three standard deviations below the mean from 10°S-30°S
167 near 30 hPa. The upward mean vertical wind anomalies are over two standard deviations above
168 the mean on the poleward side of the stream function anomaly. This upward anomaly does not
169 correspond to an actual upward circulation but expresses the weaker downward circulation than
170 average as seen in the nearly horizontal stream function regions in Fig. 3c.

171 **4 Conclusions**

172 Anomalous temperatures and circulation patterns analyzed by MERRA-2 in the southern
173 hemisphere during June 2022 can be forensically attributed to the stratospheric water vapor
174 injection from the January 2022 eruption of the Hunga Tonga-Hunga Ha'apai underwater
175 volcano. These anomalies can be traced back to March 2022. Their consistency in space and time
176 suggests a realistic response to a geophysical event rather than a yearly random dynamical
177 fluctuation. In June the record winds are part of an unusual secondary jet maximum at 10 hPa,
178 30°S-20°S.

179 These wind and temperature anomalies (Fig. 3a, b) develop from the assimilation of data, mainly
180 routine, satellite based, nadir viewing radiometers and geostrophic balance and are likely to be
181 very realistic. Note that MERRA-2 does assimilate MLS temperatures, but only at pressures of
182 5hPa and lower. The residual mean circulation might be more difficult to interpret. If the cooling
183 analysis temperature increments mainly reflect the missing water vapor cooling then they can be
184 considered to be the missing cooling term from the lack of stratospheric water vapor in the
185 assimilation system. Then the calculated residual circulation (Fig. 3c, d, e) should realistically
186 capture the perturbed residual circulation. If, however, the analysis temperature increments also
187 contain cooling induced by circulations in the atmosphere's response to the water vapor
188 perturbation, then it is possible that the residual circulation may adjust in an unphysical manner.
189 However, the good SH 20 hPa agreement between MERRA-2 and M2-SCREAM seen in the
190 sum of the analysis and radiative temperature tendencies (Fig. 2) suggests that the MERRA-2
191 analysis tendencies are representative of the missing water vapor cooling. Future work is planned
192 for model simulations that include a realistic representation of the stratospheric water
193 perturbations. These calculations should provide a more complete picture of the atmospheric
194 response to the volcanic perturbation.

195 **Acknowledgments**

196 This work was supported by NASA MAP and ACMAP programs. Resources supporting this
197 work were provided by the NASA High-End Computing (HEC) Program through the NASA
198 Center for Climate Simulation (NCCS) at Goddard Space Flight Center.

199 **Open Research**

200 The MERRA-2 products are available on the NASA Goddard Earth Sciences Data and
201 Information Services Center (GES DISC). Specific MERRA-2 product collections used here are
202 cited appropriately in the references. The 2022 temperature tendencies from M2-SCREAM are
203 available from [https://gmao.gsfc.nasa.gov/gmaoftp/STRATOSPHERE/M2-SCREAM/T-](https://gmao.gsfc.nasa.gov/gmaoftp/STRATOSPHERE/M2-SCREAM/T-tendencies/)
204 [tendencies/](https://gmao.gsfc.nasa.gov/gmaoftp/STRATOSPHERE/M2-SCREAM/T-tendencies/). Historical M2-SCREAM output can be accessed from
205 <https://disc.gsfc.nasa.gov/datasets?keywords=m2-scream&page=1>.
206

207 **References**

208

209 Andrews, D. G., Holton, J. R., and Leovy, C. B. (1987), *Middle Atmosphere Dynamics*,
210 Academic Press, 489pp.

211

212 Carr, J. L., Horváth, Á., Wu, D. L., & Friberg, M. D. (2022). Stereo plume height and motion
213 retrievals for the record-setting Hunga Tonga-Hunga Ha'apai eruption of 15 January 2022.

214 *Geophysical Research Letters*, 49, e2022GL098131. <https://doi.org/10.1029/2022GL098131>

215

216 Gelaro, R., McCarty, W., Suárez, M. J., Todling, R., Molod, A., Takacs, L., Randles, C. A.,
217 Darmenov, A., Bosilovich, M. G., Reichle, R., Wargan, K., Coy, L., Cullather, R., Draper, C.,
218 Akella, S., Buchard, V., Conaty, A., da Silva, A. M., Gu, W., Kim, G., Koster, R., Lucchesi, R.,
219 Merkova, D., Nielsen, J. E., Partyka, G., Pawson, S., Putman, W., Rienecker, M., Schubert, S.

220 D., Sienkiewicz, M., & Zhao, B. (2017). The Modern-Era Retrospective Analysis for Research
221 and Applications, Version 2 (MERRA-2), *Journal of Climate*, 30(14), 5419-5454. Retrieved Jul

222 27, 2022, from <https://journals.ametsoc.org/view/journals/clim/30/14/jcli-d-16-0758.1.xml>

223 Gille, J.C., and L.V. Lyjak (1986). Radiative Heating and Cooling Rates in the Middle
224 Atmosphere. *J. Atmos. Sci.*, 43(20), 2215-2229. DOI: <https://doi.org/10.1175/1520->
225 [0469\(1986\)043<2215:RHACRI>2.0.CO;2](https://doi.org/10.1175/1520-0469(1986)043<2215:RHACRI>2.0.CO;2)
226
227 Global Modeling and Assimilation Office (GMAO) (2022), M2-SCREAM: 3d,3-
228 Hourly,Instantaneous,Model-Level,Assimilation,Assimilated Constituent Fields,Replayed
229 MERRA-2 Meteorological Fields, Greenbelt, MD, USA, Goddard Earth Sciences Data and
230 Information Services Center (GES DISC), Accessed: July 2022, doi:10.5067/7PR3XRD6Q3NQ
231
232 Global Modeling and Assimilation Office (GMAO) (2015a), MERRA-2 instM_3d_asm_Np:
233 3d,Monthly mean,Instantaneous,Pressure-Level,Assimilation,Assimilated Meteorological Fields
234 V5.12.4, Greenbelt, MD, USA, Goddard Earth Sciences Data and Information Services Center
235 (GES DISC), Accessed: **Jul 27, 2022**, [10.5067/2E096JV59PK7](https://doi.org/10.5067/2E096JV59PK7)
236
237 Global Modeling and Assimilation Office (GMAO) (2015b), MERRA-2 tavgM_3d_tdt_Np:
238 3d,Monthly mean,Time-Averaged,Pressure-Level,Assimilation,Temperature Tendencies
239 V5.12.4, Greenbelt, MD, USA, Goddard Earth Sciences Data and Information Services Center
240 (GES DISC), Accessed: **Jul 27, 2022**, [10.5067/VILT59HI2MOY](https://doi.org/10.5067/VILT59HI2MOY)
241
242 Levelt, P. F., van den Oord, G. H. J., Dobber, M. R., Mälkki, A., Visser, H., Vries, J. D.,
243 Stammes, P., Lundell, J. O. V., and Saari, H. (2006). The Ozone Monitoring Instrument, *IEEE*
244 *Trans. Geosci. Remote Sens.*, 44, 1093–1101, <https://doi.org/10.1109/TGRS.2006.872333>.
245

246 Levelt, P. F., Joiner, J., Tamminen, J., Veefkind, J. P., Bhartia, P. K., Stein Zweers, D. C.,
247 Duncan, B., et al. (2018). The Ozone Monitoring Instrument: overview of 14 years in space,
248 *Atmos. Chem. Phys.*, 18, 5699-5745, <https://doi.org/10.5194/acp-18-5699-2018>.
249

250 Livesey, N. J., Read, W. G., Wagner, P. A., Froidevaux, L., Lambert, A., Manney, G. L. et al.
251 (2020). Version 4.2x Level 2 and 3 data quality and description document, JPL D-33509 Rev. E.
252 Retrieved from https://mls.jpl.nasa.gov/data/v4-2_data_quality_document.pdf, 2020
253

254 McCarty, Will, Lawrence Coy, Ronald Gelaro, Albert Huang, Dagmar Merkova, Edmond B.
255 Smith, Meta Seinkiewicz, and Krzysztof Wargan (2016). MERRA-2 Input Observations:
256 Summary and Assessment. NASA Technical Report Series on Global Modeling and Data
257 Assimilation, NASA/TM-2016-104606, Vol. 46, 61 pp. Document (3553 kB).
258

259 Millán, L., Santee, M. L., Lambert, A., Livesey, N. J., Werner, F., Schwartz, M. J., et al.
260 (2022). The Hunga Tonga-Hunga Ha'apai Hydration of the Stratosphere. *Geophysical Research*
261 *Letters*, 49, e2022GL099381. <https://doi.org/10.1029/2022GL099381>
262

263 Sellitto P, Podglajen A, Belhadji R, et al. The unexpected radiative impact of the Hunga Tonga
264 eruption of January 15th, 2022. Research Square; 2022. DOI: 10.21203/rs.3.rs-1562573/v1.
265

266 Wargan, K., Weir, B., Manney, G. L., Cohn, S. E., K.E. Knowland, P. Wales & Livesey, N. J.
267 (2022). M2-SCREAM: A Stratospheric Composition Reanalysis of Aura MLS data with
268 MERRA-2 transport. *Earth Sys. Sci. Dat.*, submitted.

269

270 Wargan, K., Weir, B., Manney, G. L., Cohn, S. E., & Livesey, N. J. (2020). The anomalous
271 2019 Antarctic ozone hole in the GEOS Constituent Data Assimilation System with MLS
272 observations. *Journal of Geophysical Research: Atmospheres*, 125,
273 e2020JD033335. <https://doi.org/10.1029/2020JD033335>.

274

275 Waters, J. W., Froidevaux, L., Harwood, R.S., Jarnot, R.F., Pickett, H.M., Read, W.G. et al.
276 (2006). The Earth Observing System Microwave Limb Sounder (EOS MLS) on the Aura
277 satellite. *IEEE Trans. Geosci. Remote Sens.*, 44, 1075–1092.
278 <https://doi.org/10.1109/TGRS.2006.873771>.

279

280 Xu, J., Li, D., Bai, Z., Tao, M., Bian, J. (2022) Large Amounts of Water Vapor Were Injected
281 into the Stratosphere by the Hunga Tonga–Hunga Ha’apai Volcano Eruption. *Atmosphere*, 13,
282 912. <https://doi.org/10.3390/atmos13060912>.

283